SIMULATION ANALYSIS AND EXPERIMENTAL STUDY OF SOYBEAN SEED MOTION CHARACTERISTICS IN THE SEED SUPPLY PIPELINE OF A PNEUMATIC PLANTER / 气吸式排种器供种管道内大豆种子运动特性仿真分析与试验研究

Jianqiao WANG [1,2], Kexin XU [1], Jie HAN [3], Yulong CHEN *[1,2]
[1] College of Agricultural Engineering and Food Science, Shandong University of Technology, Zibo / China
[2] Institute of Modern Agricultural Equipment, Shandong University of Technology, Zibo / China
[3] Binzhou Polytechnic, Binzhou / China
E-mail: 56565uu@sina.com
Corresponding author: Yulong Chen
DOI: https://doi.org/10.35633/inmateh-78-114

Keywords: *pneumatic central-seed-supply system, seed supply pipeline, CFD-DEM coupling, seed motion characteristics*

ABSTRACT

This study is aimed at addressing the issues of poor conveying stability, seed damage, and high energy consumption in pneumatic seeders by systematically analyzing the impact of pipeline geometry on seed motion characteristics, integrating the coupled Computational Fluid Dynamics and Discrete Element Method (CFD-DEM) simulations with bench tests. The findings demonstrate that a 45 mm pipeline diameter provides the best overall conveying performance, decreasing system pressure loss by 18.8% relative to a 40 mm diameter and increasing system pressure loss by 2.2% relative to a 50 mm diameter. The first straight section of 0.4 meters was found to provide the optimal balance between seed conveying velocity and collision protection during turns. The implementation of an arc-shaped turning structure with a 100 mm radius decreased the seed supply time to 9.48 seconds. This structure also demonstrated notably superior seed trajectory stability, improving by 26.2%, and enhanced flow field uniformity compared to polyline turn structures. This research gives important parametric guidance and theoretical support for the low-damage, high-efficiency design of pneumatic precision seeding systems.

摘要

本研究旨在通过系统分析管道几何形状对种子运动特性的影响，结合耦合计算流体动力学与离散元法（CFD-DEM）仿真与台架试验，解决气力式播种机存在的输送稳定性差、种子损伤大及能耗高的问题。研究结果表明，采用 45 毫米管径可获得最佳综合输送性能，与 40 毫米管径相比，系统压力损失降低了 18.8%；与 50 毫米管径相比，仅增加了2.2%，但。首段0.4 米直管段在种子输送速度与转弯处碰撞防护之间达到了最佳平衡。采用半径为 100 毫米的圆弧形转弯结构，将供种时间缩短至 9.48 秒。与折线形转弯结构相比，该结构在种子轨迹稳定性方面表现显著更优，提升了 26.2%，并提高了流场均匀性。本研究为气力式精量播种系统的低损伤、高效率设计提供了重要的参数指导和理论支持。

INTRODUCTION

Precision seeding technology is a key factor in achieving high-yield and efficient crop production *(Luo et al., 2016)*. The performance of the seed drill directly affects the final seeding quality *(Li et al., 2014)*. Modern large-scale seed drills often use a single central seed hopper to replace traditional multiple distributed hoppers *(Yang et al., 2022)*, which simplifies the overall machine structure and improves operational efficiency. In such systems, pneumatic seed delivery technology has become a core solution for high-speed precision seeding due to its advantages like high conveying efficiency, simple mechanical structure, and relatively low operational cost *(Qi et al., 2014)*. Therefore, air-suction seed metering devices compatible with pneumatic delivery systems are a research focus in the precision seeding field *(Zhang et al., 2016)*.

Extensive research on pneumatic central seed supply systems has been done, which includes system application, component optimization, and mechanistic analysis. To tackle the problem of uneven seed distribution, studies mainly focus on innovative distributor designs. For example, *Kumar et al., (2000),* showed that streamlined distributors improve airflow field and enhance distribution consistency, and *Li et al., (2022),* proposed a bionic distributor design.

Regarding key parameters and components, *Yatskul et al., (2017),* systematically analyzed the impact of air pressure and airflow velocity on uniformity, while *Lei Xiaolong et al., (2015),* clarified the effects of Venturi tube structural parameters on gas-solid mixing and seed motion. Coupled CFD-DEM simulation has become a crucial approach for uncovering the microscopic mechanisms underlying gas-solid two-phase flow in tubes *(Sun et al., 2026). Guzman et al., (2020),* employed this technique to investigate the interrelationships among seed forces, collisions, and airflow parameters. *Li et al., (2020), Mudarisov et al. (2020),* numerically simulated the two-phase "air sowing" flow in a grain planter shunt system. *Mangus et al., (2017),* confirmed the reliability of this simulation approach by taking high-speed camera recordings a reference. *Zhou et al., (2017),* systematically studied the influence of particle shape and swirl intensity on the erosion of elbows in pneumatic conveying.

However, existing research mainly focuses on distributors, mixing components, and macroscopic parameters. There is a lack of systematic research on how the geometric structure of the seed delivery pipeline affects seed trajectory, collision energy consumption, and conveying stability. By considering pipeline diameter, the length of the initial straight section, and the type and dimensions of turning structures as key variables, this study systematically explores how these parameters affect the internal flow field, seed movement, collision patterns, and conveying stability through theoretical analysis, coupled CFD-DEM simulations, and bench tests. The purpose is to offer a theoretical framework for pipeline optimization design and performance improvement.

MATERIALS AND METHODS

Overall System Design and Pipeline Parameter Design

The structure of the pneumatic central seed supply system for the precision planter is shown in Fig. 1, consisting of five core components: the central seed hopper, positive-pressure blower, seed distributor, seed supply pipelines, and pressure relief devices. The system is mounted on the planter frame with the following layout: the central seed hopper is positioned on the frame's drawbar and connected at its bottom to the seed distributor. The seed supply pipelines run along the main beam of the frame and are symmetrically arranged to connect to the pressure relief device of each seeding unit. Each pressure relief device interfaces directly with the seed chamber inlet of a precision seed meter. Driven by the tractor's PTO output shaft, the positive-pressure blower supplies the conveying airflow for the system.

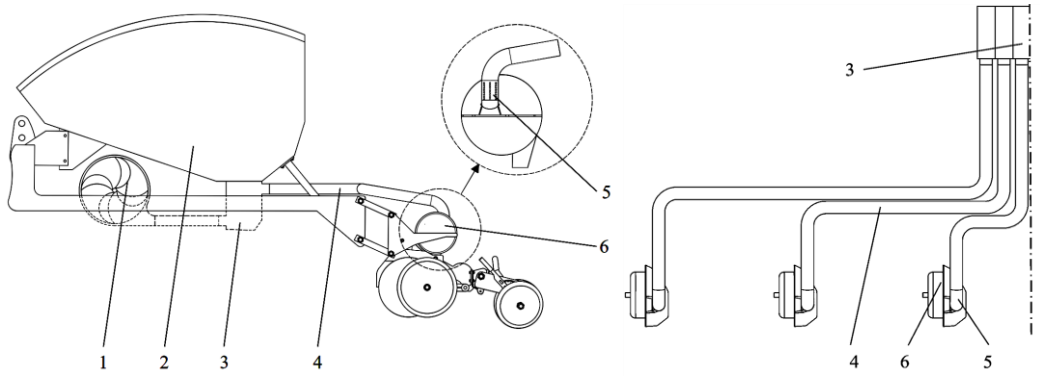

Fig. 1 - Overall schematic diagram of the central-seed-supply system
a) Front view; b) Top structural view
1. Positive-pressure blower; 2. Central seed hopper; 3. Seed distributor; 4. Seed supply pipeline; 5. Pressure relief device; 6. Seed meter.

This system employs positive pressure airflow as the medium for seed delivery. During operation, the seed population is mixed with positive pressure airflow in the distributor's mixing chamber to create a seed-air two-phase flow. The two-phase flow travels through supply pipelines, which include two bends, to reach seeding unit. Upon reaching a unit's pressure relief device, seeds and a small portion of airflow enter the seed chamber of the seed meter, while much of the airflow is vented through the device's relief ports, thus achieving remote seed supply. In this system, the supply pipelines are responsible for distributing seed-air mixture from the central distribution point to each seeding endpoint.

According to the particle conveying theory applicable to seed delivery pipes *(Zhang et al., 2024)*, the calculation of inlet air velocity proceeds as follows:

$$v_g = k_L\sqrt{\rho_P} + k_d L_G \text{ [m/s]} \quad (1)$$

where:

v_g is the inlet air velocity, [m/s]; k_L is the particle size coefficient, [m^{4}s^{-1}kg^{-2}]; ρ_p is the particle density, ×10^3 [kg/m^3]; k_d is the material characteristic coefficient, [s^{-1}]; L_G is the pipe length, [m].

The total system pressure loss (P_C) is the sum of losses from individual components, primarily including the distributor loss, frictional loss along the pipeline, and the local loss from the 90° bends. The distributor loss (P_v) was measured experimentally in a prior study as 1147.34 Pa.

The pressure loss in the seed supply pipeline (P_p) is primarily due to airflow friction, calculated as:

$$P_p = \lambda \frac{L_P}{D_P} \rho_g \frac{v_g^2}{2} \text{ [Pa]} \quad (2)$$

λ is the friction factor, calculated using the Blasius formula:

$$\lambda = 0.0125 + \frac{0.00011}{D_P} \quad (3)$$

where:

The pipeline length L_P taken as 1.3 m, pipe diameter D_P taken as 0.045 m, λ is 0.01494, ρ_g is the density of air, which is 1.205 kg/m^3 under one standard atmospheric pressure, P_p = 148.92 Pa.

$$P_e = \xi \rho_g \frac{v_g^2}{2} \text{ [Pa]} \quad (4)$$

where:

ξ is the coefficient of air pressure loss for the bend. Given that the Reynolds number (Re) in the supply pipeline satisfies Re > 3 × 10^5, the coefficient is determined by

$$\xi = 0.00431 c\psi Re^{-0.17} \left(\frac{R}{D_P}\right)^{0.84} \quad (5)$$

where:

ψ is the bend angle (90° in this study), ξ is 0.12, Pe = 38.24 Pa.

$$P_C = P_v + P_p + 2P_e = 1372.74 \text{ [Pa]} \quad (6)$$

where:

The required airflow rate at the system inlet (Q_C), related to the inlet velocity and pipe diameter, is calculated as:

$$Q_C = 900 v_g \pi D_P^2 \text{ [m}^3\text{/h]} \quad (7)$$

where:

Calculation based on the data indicated that the required airflow rate at the inlet of the central seed supply system is 131.68 m³/h, with a required pressure of no less than 1372.74 Pa.

Soybean seed geometry and material properties

Soybean seeds (*cultivar Zhonghuang 37*) were selected as the research material. One hundred seeds were randomly sampled for measurements, including dimensions, airflow suspension velocity, moisture content, and thousand-seed weight. The seed length, width, and thickness were measured using a vernier caliper with an accuracy of 0.2 mm. The dimensional distribution is presented in Fig. 2. The average values for these triaxial dimensions were 7.83 mm, 7.02 mm, and 6.04 mm, respectively.

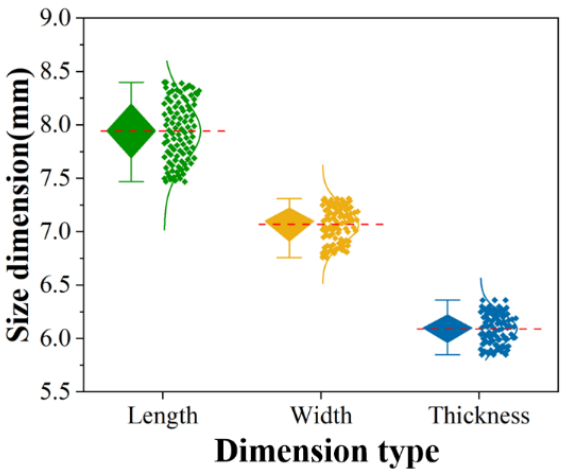

Fig. 2 - Triaxial dimensions of soybean seeds

Based on the measured triaxial dimensions, the equivalent diameter of the Zhonghuang 37 soybean seeds is calculated using Equations (8).

$$D_s = \sqrt[3]{l \cdot w \cdot t} \text{ [mm]} \quad (8)$$

where:

l is the length of seeds, [mm]; w is the width of seeds, [mm]; t is the thickness of seeds, [mm].

The sphericity of seeds is the degree of difference between the actual shape of the seed and the ball. The average sphericity of soybean seeds is calculated according to the Equations (9).

$$S_p = \frac{D_s}{l} \times 100\% \quad (9)$$

where: the calculated equivalent diameter Ds is 6.92 mm, and the sphericity Sp is 88.39%.

Suspension velocity is an important hydrodynamic property of material particles, which refers to the fluid velocity when material particles are suspended in fluid, is used in material conveying and material separation *(Su et al., 2016)*. Determining the suspension velocity through theoretical derivation proved difficult for the seed population, so it was instead established experimentally using a material suspension test rig *(Liu et al., 2016).* During testing, random soybean samples were placed upward from the bottom of a conical tube. The airflow velocity inside the tube was adjusted so that the seeds reached a stable suspended state. The corresponding airflow velocity and suspension height were recorded, and the suspension velocity was calculated by using the calibrated L-K curve of the equipment. The average value from repeated tests for Zhonghuang 37 soybean seeds is 11.43 m/s. Additional key material properties were measured: the weight of 248.109 g was determined by an electronic analytical balance with a resolution of 0.01 g; the moisture content was 8.5%, measured with a near-infrared grain analyzer. These parameters together offer the key material property basis.

The Development of the CFD-DEM Coupled Simulation Model

The layout of the seed supply pipeline can be simplified into a model consisting of three straight sections and two bends, as shown in Fig. 3. The first and second straight sections, l_1 and l_2 are positioned horizontally, whereas the third straight section, l_3, is inclined at roughly 15° to the horizontal plane to accommodate the mounting needs of the seed meters. According to the 50 mm row spacing, the six seeding units of the planter are divided into three groups: outermost row, sub-outer row, and middle row. The second horizontal pipeline section l_2 for these groups has corresponding lengths of 1.1 m, 0.65 m, and 0.2 m, respectively. The third section l_3 has a length of 0.3 m.

To systematically analyze the influence of pipeline structure on internal flow field and seed motion characteristics, this study investigates the following parameters via simulation: pipeline diameter at three levels of 40 mm, 45 mm, 50 mm; length of the first straight section l_1 at four levels of 0.2 m, 0.4 m, 0.6 m, 0.8 m; and turning structure type comparing arc-shaped and polyline forms, with their key dimensions, like arc radius and polyline width, both selected at three levels of 50 mm, 75 mm, 100 mm. This parametric study is to optimize the pipeline design, so that the conveying stability and operational efficiency improve.

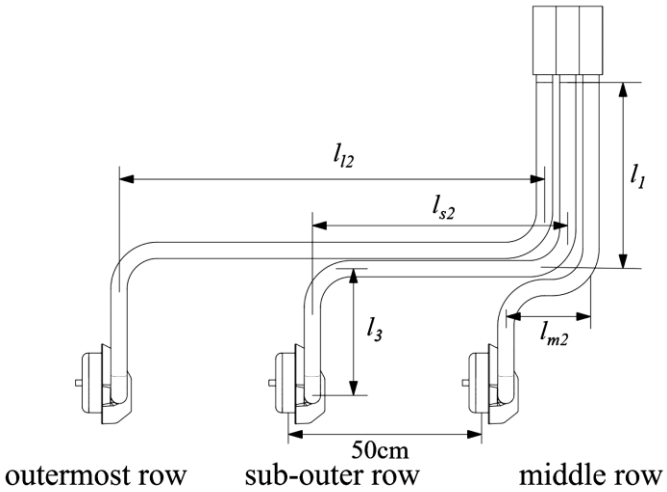

Fig. 3 - Seed supply pipeline arrangement

To achieve the computational stability requirements *(Qian et al., 2025).* for the coupled CFD-DEM simulation and accurately model the non-spherical soybean seeds, this study used the clump method to build the particle model. According to the three-dimensional contour of the seeds, this method creates a particle cluster that is equivalent to the real seed in both geometry and mechanical properties by bonding miniature spherical particles. This method guarantees simulation accuracy and enhances modeling efficiency.

To perform the coupled simulation, an integrated geometric model was developed that includes both the distributor outlet and the seed supply pipeline, which were then meshed together to define the fluid domain. In the Fluent simulation, the fluid boundary conditions were defined with two airflow inlets assigned velocities of 14.88 m/s and 14.55 m/s, respectively, while the outlet was configured to maintain atmospheric pressure. A transient pressure-based solver was used, which employs the Realizable k-ε turbulence model, and the air properties are defined under standard conditions. This mesh model was imported into EDEM to become the discrete element calculation domain. A particle factory was established at the pipeline entrance, producing bonded particle clusters at a rate of 500; per second to mic the soybean seed population. Based on previous flow field analysis, the initial particle velocity was set at X: 1.182 m/s and Y: -0.2084 m/s. Table 1 presents the contact mechanical parameters between particles and the pipeline. To guarantee the coupled calculation remains stable, the EDEM time step was set to 5×10^{-7} seconds, and the Fluent time step was set to 5×10^{-5} seconds, keeping a factor of 100; between them. The gas-solid two-phase flow coupling was achieved through a two-way coupling interface.

Table 1

Discrete element simulation parameters

Category	Parameter	Value
Soybean	Poisson's ratio	0.4
	Shear modulus [Pa]	1.1×107
	Density [kg/m³]	1211.30
Rubber pipeline	Poisson's ratio	0.35
	Shear modulus [Pa]	1.2×10^{8}
	Density [kg/m³]	1454.7
Coefficient of restitution	Soybean-Soybean	0.41
	Soybean-Rubber pipeline	0.52
Static friction coefficient	Soybean-Soybean	0.60
	Soybean-Rubber pipeline	0.45
Rolling friction coefficient	Soybean-Soybean	0.044
	Soybean-Rubber pipeline	0.040

Bench Test Design

To validate the simulation results and investigate the actual influence of the pipeline and pressure relief structure on seed supply performance, a dedicated test bench was constructed as shown in Fig. 4. The central seed supply system requires an airflow rate of 131.68 m³/h and a pressure not less than 1372.74 Pa at its inlet. To ensure adequate air velocity and pressure, a 10% margin was added to the airflow requirement. Therefore, an XGB-1500 high-pressure vortex blower (Taizhou Yinan Electromechanical Co., Ltd.) was selected, with a power rating of 1500 W, a maximum flow rate of 250 m³/h, and a maximum positive pressure of 32 kPa.

The bench primarily consists of the blower with its frequency converter, a seed distributor, a FASTCAM Mini AX high-speed camera system, seed supply pipelines, a supplementary lighting system, pressure relief devices, and a data-acquisition computer. Transparent PVC hoses with embedded steel wires were used for the seed supply pipelines; this material provides sufficient stiffness while allowing clear observation of seed motion. The high-speed camera was employed to record the trajectory of seeds inside the turning structures and to capture images directly through the transparent side wall of the distributor for accurate measurement of the seed supply time. The seed supply time was defined as the time interval from the first frame where seed movement was observed at the distributor outlet to the frame where seeds first appeared at the pipeline outlet.

The recording duration was set to 20 s at a speed of 250 frames per second (fps). High-speed image processing was performed using the FASTCAM Mini AX system's proprietary software. Each video was analyzed frame-by-frame.

To analyze the effects of pipeline structure and pressure relief structure on the performance of the central seed supply system, and to validate the rationality of the CFD-DEM coupled simulation, experiments were conducted to investigate the influence of the pipeline turning structure and the pressure relief structure on seed supply performance. The seed supply pipeline connected to the sub-outer row seeding unit was selected as the test object. The length of the first pipeline section was set to 0.4 meters. Two kinds of turning structures were tested, namely arc-shaped and polyline. For each type, three dimensions were analyzed: the arc radii (50 mm, 75 mm, 100 mm).

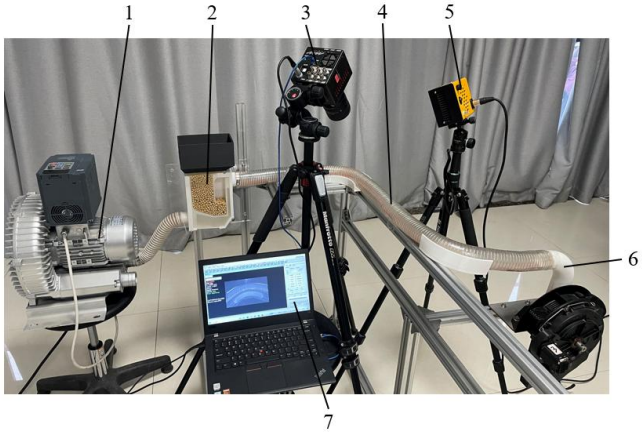

Fig. 4 - Test bench for seed supply performance

1. Blower and frequency converter; 2. Seed distributor; 3. High-speed camera; 4. Seed supply pipeline; 5. Supplementary light; 6. Pressure relief device; 7. Computer

The supply time of seeds and the coefficient of variation (CV) served as metrics for evaluating supply performance. The seed supply time refers to the time span from when the seed population in the distributor's mixing chamber starts from a stationary condition to when it becomes fluidized and ready for conveyance. The testing involved repeating each combination three times, yielding six test groups in total (two structural types multiplied by three dimensions). For each group, the average seed supply time and its coefficient of variation were computed.

In each repeated test, 500 soybean seeds were manually introduced into the seed distributor's mixing chamber. All bench tests were conducted under controlled indoor environmental conditions: ambient temperature of 25 °C and relative humidity of 52% RH.

CV for seed supply time was calculated as:

$$CV = \frac{\delta}{t} \times 100\% \quad (10)$$

where: δ is the standard deviation of the three repeated measurements; t is the average seed supply time [s].

RESULTS

Analysis of Simulation Results on the Influence of Pipe Diameter on Seed Motion Characteristics

The airflow field and seed motion parameters under different pipe diameters are compared in Table 2. As the diameter increased from 40 mm to 50 mm, the resultant force on the seeds at the outlet, the airflow velocity, the seed velocity, and the relative velocity between the gas and solid phases all exhibited a decreasing trend, indicating that a larger pipe diameter reduces the conveying kinetic energy of the seeds.

Table 2

Effect of pipe diameter on airflow field and seed movement

Pipe diameter	Force	Airflow Velocity	Seed Exit Velocity	Relative Velocity	Pressure Loss
[mm]	[N]	[m/s]	[m/s]	[m/s]	[Pa]
40	8.27×10^{-4}	17.82	4.94	12.88	888.01
45	7.84×10^{-4}	14.22	3.99	10.23	721.42
50	6.65×10^{-4}	11.69	3.18	8.51	705.23

Meanwhile, the pressure loss in the pipe also reduced, reaching a minimum of 721.42 Pa at a diameter of 45 mm. As the pipe diameter increased, the maximum seed velocity within it decreased, while the seeds' spatial distribution grew denser, as depicted in Fig.5. The 45 mm diameter offered a relatively low pressure loss and gas-solid relative velocity. This finding is in line with theoretical analysis and meets the standards for efficient and stable soybean seed conveying.

a) *b)* *c)*

Fig. 5 - The distribution of seeds according to different pipe diameters

a) Pipe diameter: 40 mm; b) Pipe diameter: 45 mm; c) Pipe diameter: 50 mm

Analysis of Simulation Results regarding the Impact of Turning Structure Type and Dimensions on Seed Motion Characteristics

The geometric parameters of the turning structure have an impact on the airflow distribution and seed motion characteristics. The force on seeds at the pipeline outlet decreased as the arc radius or polyline width increased, as shown in Table 3. For a polyline width of 50 mm, the highest resultant force and airflow velocity were observed, and the optimal outlet seed velocity and relative gas-solid two-phase flow velocity were achieved with an arc radius of 100 mm. The pressure drop across the turning structure decreased by 8.3% (1489) when larger arc radii were used, but increased with wider polyline dimensions.

Table 3

Effect of steering structure on airflow field and seed movement

Arc radius	Polyline Width	Force	Airflow Velocity	Seed Exit Velocity	Relative Velocity	Pressure Loss
[mm]	[mm]	[N]	[m/s]	[m/s]	[m/s]	[Pa]
50	/	8.49×10^{-4}	14.22	3.99	10.23	26.68
75	/	7.89×10^{-4}	14.29	3.55	10.74	23.08
100	/	7.08×10^{-4}	14.13	4.11	10.02	19.72
/	50	9.02×10^{-4}	14.45	3.97	10.48	15.88
/	75	8.62×10^{-4}	14.09	3.74	10.35	19.75
/	100	7.95×10^{-4}	14.08	3.55	10.53	33.12

The airflow distribution for different turning structures is shown in Fig. 6. The arc-shaped turning structures exhibited superior uniformity in airflow velocity distribution compared to the polyline turning structures. The airflow velocity distribution for arc radii of 75 mm and 100 mm was more uniform than that for a 50 mm radius. Furthermore, for arc radii of 75 mm and 100 mm, the airflow distributions at the cross-sections before and after the turn were similar. Regarding pressure distribution, the structure with a 100 mm arc radius demonstrated greater uniformity than those with 50 mm and 75 mm radius, and also outperformed the polyline turning structures.

The seed distribution states across various turning structures is shown in Fig. 7. As seeds moved through the turning section, the decrease in their velocity attenuation became less pronounced with increases in the radius of arcs or the width of polylines in the turning structure, leading to a smaller loss in seed kinetic energy.

In the arc-shaped turning structures, the overall trajectory of seeds in the pipeline remained relatively stable, with a conveying rate of 6.0% (1084). In the straight sections of the supply pipeline, the seed flow is denser near the pipe bottom, and most seeds are transported by rolling along the bottom. At both turning sections, seeds usually moved along the outer wall of the turning structure. This behavior is due to the inertia of the seeds. Seeds that first collided with the outer wall of the arc in a straight-line motion were affected by airflow, resulting in their reflection trajectory angle becoming smaller than the geometric reflection angle. Therefore, these seeds collided with the outer wall before leaving the arc structure.

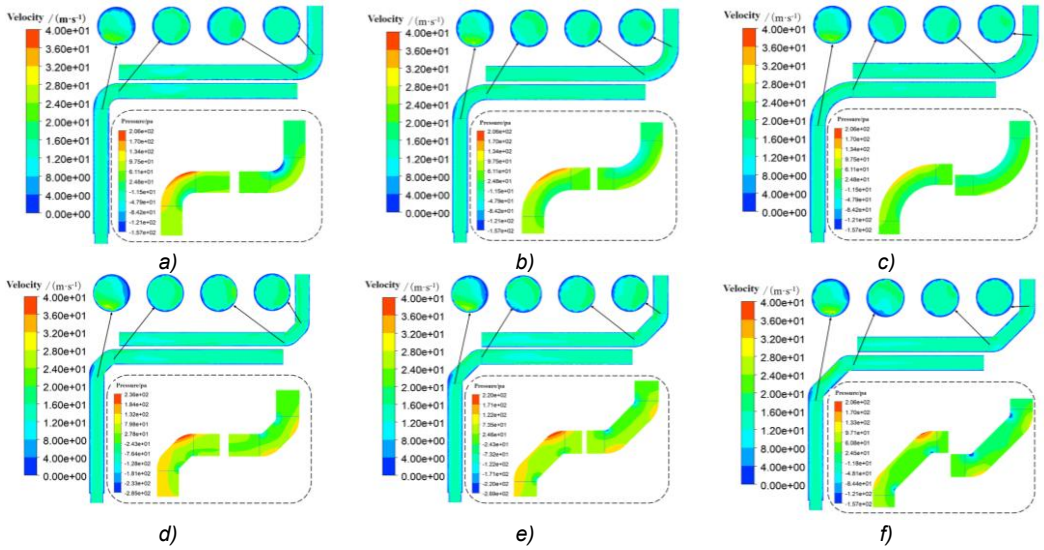

Fig. 6 - Airflow distribution of different steering structures
a) Arc radius: 50 mm; b) Arc radius: 75 mm; c) Arc radius: 100 mm
d) Polyline width: 50 mm; e) Polyline width: 75 mm; f) Polyline width: 100 mm

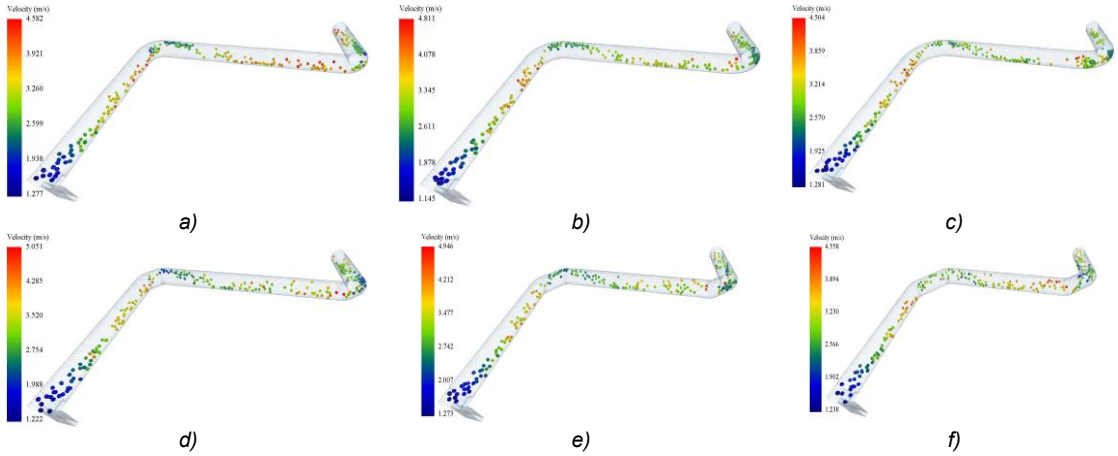

Fig. 7 - Seed distribution state of different steering structures
a) Arc radius: 50 mm; b) Arc radius: 75 mm; c) Arc radius: 100 mm;
d) Polyline width: 50 mm; e) Polyline width: 75 mm; f) Polyline width: 100 mm

Based on the seed distribution patterns, the degree of collision between seeds and the pipe wall within the turning structure decreased as the arc radius increased. In polyline turning structures, the conveying trajectories of seeds within the pipeline were more dispersed, with higher uniformity and more pronounced influence from the airflow. Consequently, in the straight sections of pipelines with polyline turns, seed velocities were higher compared to those in arc-shaped turn pipelines. During the seed supply process, when seeds collided with the polyline turning structure, the attenuation of their velocity was more pronounced than with arc-shaped turns. Within the supply pipeline, seeds moved close to the bottom along the pipeline axis, primarily driven by fluid drag force. Overall, the pipeline with a 100 mm arc radius exhibited uniform flow velocity distribution, lower pressure loss, and less deceleration in seed motion.

Analysis of Simulation Results on the Influence of Pipeline Layout on Seed Motion Characteristics

The airflow field characteristics and seed motion parameters for the middle-row, sub-outer-row, and outermost-row seeding units under different lengths of the first pipeline section are presented in Table 4. The integrated data analysis indicates that as the pipeline length increased from 0.2 m to 0.8 m, the airflow velocity within the system showed a gradual upward trend, accompanied by a corresponding increase in pressure loss.

Table 4

Influence of Pipeline Length on Seed Motion Characteristics

Position of the Row	lm1	Force	Airflow Velocity	Seed Exit Velocity	Relative Velocity	Pressure Loss
	[m]	[N]	[m/s]	[m/s]	[m/s]	[Pa]
middle	0.2	7.19×10^{-4}	14.27	3.81	10.46	698.11
middle	0.4	7.89×10^{-4}	14.38	3.78	10.60	707.13
middle	0.6	7.16×10^{-4}	14.50	3.67	10.83	726.53
middle	0.8	7.11×10^{-4}	14.58	3.75	10.83	728.08
sub-outer	0.2	8.86×10^{-4}	14.54	4.06	10.48	736.47
sub-outer	0.4	7.84×10^{-4}	14.22	3.99	10.23	721.42
sub-outer	0.6	8.27×10^{-4}	14.33	3.65	10.68	755.70
sub-outer	0.8	8.47×10^{-4}	14.21	3.34	10.97	780.49
outermost	0.2	8.06×10^{-4}	14.39	4.16	10.23	755.31
outermost	0.4	7.34×10^{-4}	14.25	4.35	9.90	763.25
outermost	0.6	7.21×10^{-4}	14.20	4.28	9.92	767.18
outermost	0.8	6.66×10^{-4}	14.19	4.21	9.98	771.99

Of all the lengths examined, 0.4 m exhibited the best conveying performance overall. At this specific length, the middle-row unit generated the highest resultant force on seeds, measuring 7.89×10^{-4} N. Meanwhile, the sub-outer-row unit displayed the lowest system pressure loss at 721.42 Pa. The outermost-row unit attained the highest outlet seed velocity of 4.35 m/s, accompanied by the lowest relative gas-solid two-phase flow velocity of 9.90 m/s. When compared to other lengths, a length of 0.4 m effectively balanced the enhancement of seed conveying kinetic energy and energy control loss.

The motion states of seeds across varying pipeline lengths is shown in Fig. 8.

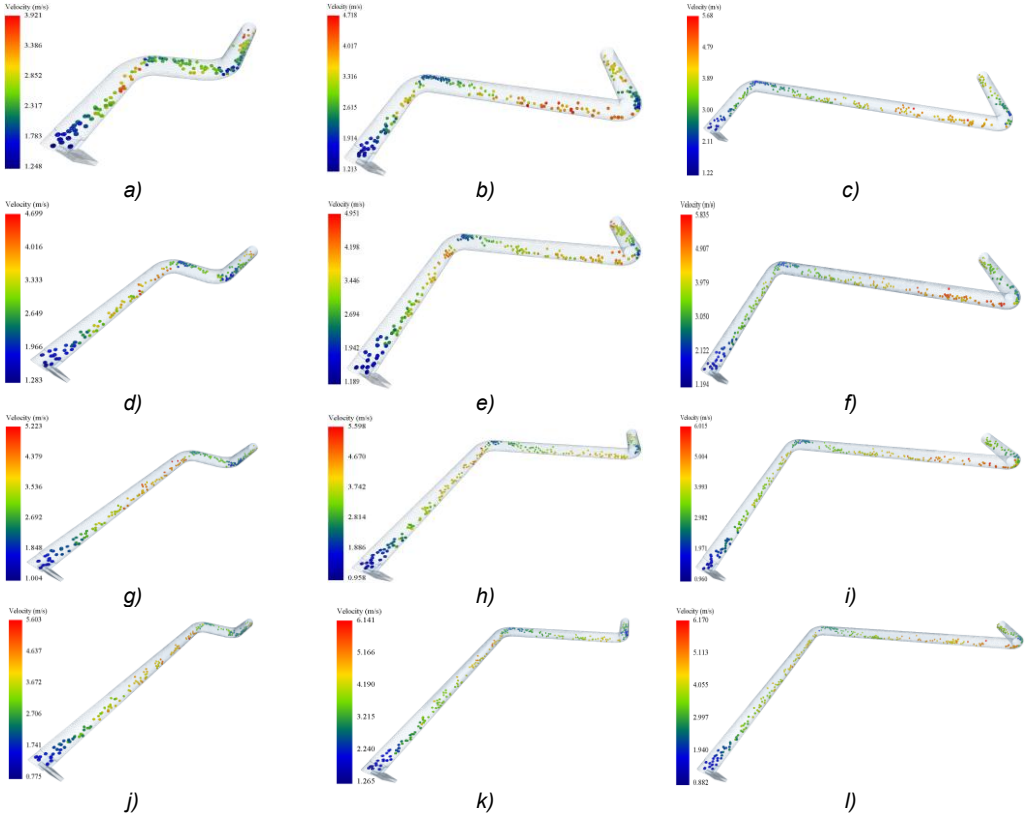

Fig. 8 - Influence of Pipeline Length on Seed Trajectories and Collisions

a) Middle row, l_{m1}=0.2m; b) Sub-outer row, l_{m1}=0.2m; c) Outermost row, l_{m1}=0.2m; d) Middle row, l_{m1}=0.4m; e) Sub-outer row, l_{m1}=0.4m; f) Outermost row, l_{m1}=0.4m; g) Middle row, l_{m1}=0.6m; h) Sub-outer row, l_{m1}=0.6m; i) Outermost row, l_{m1}=0.6m; j) Middle row, l_{m1}=0.8m; k) Sub-outer row, l_{m1}=0.8m; l) Outermost row, l_{m1}=0.8m

The results show that pipeline length has an impact on both the seed acceleration process and collision behavior during turns. When the pipeline was short, seeds had insufficient acceleration, and their maximum velocity usually happened near the turning structures or pipeline outlet. When the length reached the range of 0.4 to 0.8 m, accounting for 37.6% (6775 instances), seeds achieved more thorough acceleration in the straight section, typically reaching their peak velocity prior to entering the turns. In longer pipelines, seeds enter the turning zone at higher speeds, causing intensified collisions and more velocity loss.

For all three seeding unit types, a first straight section length of 0.4 m was used, which resulted in a seed trajectory that is relatively continuous and stable, with fewer collisions. This length achieves a balance among various performance metrics, taking into account efficient conveyance, controlled energy loss, and stable seed motion. So, it was chosen as the preferred parameter. This conclusion gives a reason to optimize the pipeline structure in pneumatic seed supply systems.

Bench Test Validation and Performance Assessment

The coupled CFD-DEM simulation model and its parameter settings were systematically validated by comparing the actual seed motion, recorded using high-speed photography during bench tests, with the corresponding simulation outcomes. As shown in Fig. 9, the seed supplying process in the pipeline captured by the high-speed camera has the same trend as the seed supplying process of the CFD-DEM coupled simulation. The CFD-DEM simulation was validated by comparing predicted seed supply times with experimental measurements, which is shown in Table 5.

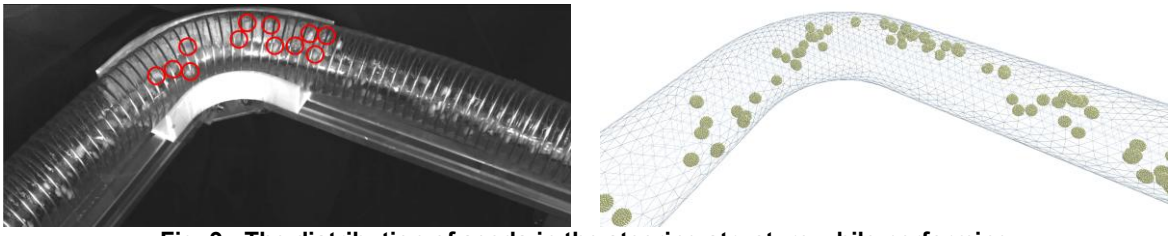

Fig. 9 - The distribution of seeds in the steering structure while performing high-speed photography and simulation

Table 5

Seed supply performance with different turning structure

Pipeline Type	Arc Radius	Polyline Width	Seed Supply Time in Bench Test	CV	Seed Supply Time in CFD-DEM Simulation	CV
	[mm]	[mm]	[s]	[%]	[s]	[%]
Arc-shaped turning structure	R=50	/	9.68	0.35	9.75	0.38
	R=75	/	9.76	0.69	9.82	0.65
	R=100	/	9.48	0.75	9.52	0.78
Polyline turning structure	/	H=50	9.34	2.10	9.92	2.05
	/	H=75	9.96	1.35	9.85	1.40
	/	H=100	9.80	1.91	9.70	1.88

Analysis indicates that seed supply time has a nonlinear trend, where the arc radius or polyline width initially increases slightly, but then decreases. The absolute differences between parameter sets were minimal, spanning only from 9.34 to 9.96 s, suggesting that structural dimensions within the examined range did not influence conveying efficiency in a straightforward linear fashion. The coefficient of variation for supply time consistently stayed under 4% across all test groups. The pipeline has a 50 mm arc radius, which shows exceptional temporal stability, with a coefficient of variation of just 0.35%. However, data from multiple repeated tests showed that the pipeline with a 100 mm arc radius doesn't just gives stable supply times, it also consistently has shorter durations compared to arcs with smaller radius. For the 100 mm arc radius (optimal configuration), the simulated supply time was 9.52 s, while the experimental value was 9.48 s, yielding a relative error of 0.4%. For all six test groups, the maximum relative error between simulation and experiment was 6.2%. Therefore, the simulation model is considered reliable for analyzing seed motion characteristics in the turning structure.

CONCLUSIONS

(1) The diameter of the pipe significantly affects the system's energy efficiency and conveying performance. According to the study, a pipe diameter of 45 mm significantly decreased system pressure loss by 18.8% compared to a 40 mm diameter and only increased by 2.2% compared to a 50 mm diameter. This demonstrates that the 45 mm diameter offers an optimal balance between conveying efficiency and energy consumption.

(2) The initial straight section's length significantly influences seed acceleration and collision dynamics during turns. A length of 0.4 m allowed seeds to achieve an appropriate initial velocity while reducing the collision intensity at the turning structures. This approach reduces the risk of mechanical damage to seeds while preserving conveying efficiency.

(3) The type and geometry of the turning structure are crucial in achieving airflow uniformity and maintaining seed motion stability. Arc-shaped turns overall show a better performance compared to polyline turns. The arc structure with a 100 mm radius demonstrated superior overall performance, recording a seed supply time of 9.48 s, maintaining stable seed trajectories, and ensuring a uniform flow field distribution, all of which facilitated stable and efficient seed conveyance.

In conclusion, the influence of pipe diameter, first section straight pipe length and turning structure on the movement characteristics of soybean seeds was systematically analyzed. However, there are still limitations such as only testing a single variety (Zhonghuang 37), testing only under indoor conditions (25±2 °C, 50±5% RH), only quantitative verification of 100 mm arc bends, and not simulating seed-seed collisions in the dispenser.

ACKNOWLEDGEMENT

The authors were funded for this project by the Shandong Province Agricultural Machinery R&D, Manufacturing, Promotion and Application Integration Pilot Project (No.NJYTHSD-202304), the High-Quality Development Special Project of the Ministry of Industry and Information Technology (No.2023ZY02009), and the Young Innovative Teams Program for Universities of Shandong Province (No.2022KJ225).

REFERENCES

[1] Guzman L., Chen Y., & Landry H. (2020). Coupled CFD-DEM Simulation of Seed Flow in an Air Seeder Distributor Tube. *Processes*, vol. 8, no. 12, 2020, pp. 1597. Basel/Switzerland. https://doi.org/10.3390/pr8121597

[2] Kumar V. J. F., & Durairaj C.D. (2000). Influence of head geometry on the distributive performance of air-assisted seed drills (头部几何形状对空气辅助播种机分布性能的影响). *Journal of Agricultural Engineering Research*, vol.75, no.1, pp.81-95. London/UK. https://doi.org/10.1006/jaer.1999.0490

[3] Lei X. L., Liao Y.T., Li Z.D., Cao X.Y., Li S. S., Wei Y. P., & Liao Q.X. (2015). Design and experiment of seed feeding device in air-assisted centralized metering device for rapeseed and wheat (油麦兼用型气送式集排器供种装置设计与试验). *Transactions of the Chinese Society of Agricultural Engineering*, vol. 31, no. 20, 2015, pp. 10-18. Beijing/China. https://doi.org/10.11975/j.issn.1002-6819.2015.20.002

[4] Li H. C., Gao F., Zhao Z., & Liu W. (2014). Domestic and overseas research status and development trend of precision seed-metering device (国内外精密排种器研究现状与发展趋势). *Journal of Chinese Agricultural Mechanization*, vol. 35, no. 2, pp. 12-16. Beijing/China. https://doi.org/10.13733/j.jcam.issn.2095-5553.2014.02.004

[5] Li Y., Zhao J., Liu L., & Liu R. (2022). Biomimetic Design and Experiment of Distributor of Pneumatic Seeding System Based on Crucian Curve (基于十字曲线的气动播种系统仿生设计与实验). *Transactions of the Chinese Society for Agricultural Machinery*, 53(2), pp. 80–87. Beijing/China. https://doi.org/10.6041/j.issn.1000-1298.2022.02.008

[6] Li Y. J., Liu Y. H., & Liu L. J. (2020). Distribution Mechanism of Airflow in Seed Tube of Different Lengths in Pneumatic Seeder (气送式播种机输种管长度影响管内气流分布的机理). *Transactions of the Chinese Society for Agricultural Machinery*, 51(06), pp. 55-64. Beijing/China. https://doi.org/10.6041/j.issn.1000-1298.2020.06.006

[7] Li Y. J., Liu R., Liu C. X., & Liu L. J. (2021). Simulation and Test of Seed Velocity Coupling in Seed Tube of Pneumatic Seed Metering Device (气送式排种器输种管内种子速度耦合仿真测定与试验). *Transactions of the Chinese Society for Agricultural Machinery*, 52(04), pp. 54-61. Beijing/China. https://doi.org/10.6041/j.issn.1000-1298.2021.04.007

[8] Liu Y. H. (2019). *Design and experiment of pneumatic balance device for pneumatic seed metering system (气流输送式排种系统气压平衡装置的设计与试验).* [Doctoral dissertation, Chinese Academy of Agricultural Mechanization Sciences, Beijing/China.]

[9] Luo X., Liao J., Hu L., Zang Y., & Zhou Z. (2016). Improving agricultural mechanization level to promote agricultural sustainable development (提升农业机械化水平，促进农业可持续发展). *Transactions of the Chinese Society of Agricultural Engineering*, 32(1), pp. 1–11. Beijing/China. https://doi.org/10.11975/j.issn.1002-6819.2016.01.001

[10] Mangus D. L., Sharda A., Flippo D., Strasser R., & Griffin T. (2017). Development of high-speed camera hardware and software package to evaluate real-time electric seed meter accuracy of a variable rate planter. *Computers and Electronics in Agriculture*, vol. 142, 2017, pp. 314-325. Amsterdam/Netherlands. https://doi.org/10.1016/j.compag.2017.09.014

[11] Mudarisov S., Badretdinov I., Rakhimov Z., Lukmanov R., & Nurullin E. (2020). Numerical simulation of two-phase air – seed flow in the distribution system of the grain seeder. *Computers and Electronics in Agriculture*, vol. 168. Amsterdam/Netherlands. https://doi.org/10.1016/j.compag.2019.105151

[12] Qi B. (2014). *Design and experimental study of central exhaust pneumatic precision seed metering device (中央排气气动精密排种装置的设计与实验研究).* [Doctoral dissertation, China Agricultural University, Beijing/China.]

[13] Qian J., Fan. Z. R., Yan. D. Q., Qin. W., Jiang. Y. C., Huang. Z. S., Xing. H., Wang. Y., & Zang. Y. (2025). Numerical simulation of dry and wet rice seeds in an air-suction seed metering device. (气吸式排种器中的干米和湿米种子数值模拟). *Agronomy*, vol. 15, no. 5, p. 1145. Basel/Switzerland. https://doi.org/10.3390/agronomy15051145

[14] Su W., Gao X. J., & Ren C. (2016). Simulation and prediction method for suspension velocity of seed particle swarm (种子颗粒群的悬浮速度模拟预测方法). *Journal of South China Agricultural University*, 37(1), pp. 110-116.

[15] Sun C., Zhang H., Ge Y., Zeng H.F., & Zheng Y.J. (2026). Dynamic characteristics analysis of pneumatic collection device for continuous harvesting of dry safflower based on CFD-DEM (基于 CFD-DEM 的干红花连续采收气动装置动态特性分析). *Computers and Electronics in Agriculture*, vol. 240, 2026, pp. 111176. Amsterdam/Netherlands. https://doi.org/10.1016/j.compag.2025.111176

[16] Yang S. P. (2022). *Design and experiment of pneumatic wheat seed metering system (气力集排式小麦排种系统设计与试验).* [Doctoral dissertation, Northwest A&F University, Haerbin/China.]

[17] Yatskul A., Lemiere J. P., & Cointault F. (2017). Influence of the divider head functioning conditions and geometry on the seed's distribution accuracy of the air-seeder. *Biosystems Engineering*, vol. 161, 2017, pp. 120–134. London/UK. https://doi.org/10.1016/j.biosystemseng.2017.06.015

[18] Zhang D. G., Lu Y. G., & Xie HX. (2016). Overview and development of pneumatic conveying technology for agricultural granular materials (农业颗粒物料气力输送技术概况与发展). *Food Industry*, 37(10), pp. 200-203.

[19] Zhang W.C. (2024). *Design and experiment of first-order pneumatic rice direct-seeding metering system. (一阶气动水稻直播计量系统的设计与试验).* [Master dissertation, Huazhong Agricultural University, Wuhan/China.]

[20] Zhou J., Liu Y., Liu S., Du C., & Li J. (2017). Effects of particle shape and swirling intensity on elbow erosion in dilute-phase pneumatic conveying (颗粒形状和旋流强度对稀相气力输送弯头冲蚀的影响). *Wear*, 380-381, 66-77. https://doi.org/10.1016/j.wear.2017.03.009